

Deformation process and prediction of filling gangue: A case study in China

Changxiang Wang^{1,2a}, Yao Lu^{*1,2}, Yangyang Li^{1,2,3b}, Buchu Zhang^{1,2c} and Yanbo Liang^{1,2d}

¹College of Mining and Safety Engineering, Shandong University of Science and Technology, Qingdao 266590, China

²State Key Laboratory of Mining Disaster Prevention and Control Co-Founded by Shandong Province and the Ministry of Science and Technology, Qingdao 266590, China

³State Key Laboratory of Water Resource Protection and Utilization in Coal Mining, China

(Received December 29, 2018, Revised June 17, 2019, Accepted July 8, 2019)

Abstract. Gangue filling in the goaf is an effective measure to control the surface subsidence. However, due to the obvious deformation of gangue compression, the filling effect deserves to be further studied. To this end, the deformation of coal gangue filling in the goaf is analyzed by theoretical analysis, large-scale crushed rock compression test, and field investigation. Through the compression test of crushed rock, the deformation behaviour characteristics and energy dissipation characteristics is obtained and analysed. The influencing factors of gangue filling and predicted amount of main deformation are summarized. Besides, the predicted equation and filling subsidence coefficients of gangue are obtained. The gangue filling effect was monitored by the movement observation of surface rock. Gangue filling can support the roof of the goaf, effectively control the surface subsidence with little influence on the ground villages. The premer and equations of the main deformation in the gangue filling are verified, and the subsidence coefficient is further reduced by adding cemented material or fine sand. This paper provides a practical and theoretical reference for further development of gangue filling.

Keywords: gangue filling; large-scale crushed rock compression test; deformation behaviour characteristics; energy dissipation characteristics; movement observation of surface

1. Introduction

In the coal mining, due to damaged stress state of original rock, surrounding rock is inevitably subject to the bottom-top failure, endangering the safety of surface buildings, people's lives and properties (Ghabraie *et al.* 2017, Ishwar and Kumar 2017, Shen and Barton 2018, Ju and Xu. 2015). Since the 21st century, coal mining has entered a new era, namely Green Mining, including water conservation mining, coal mining under buildings and subsidence reduction with grouting in the bed separation, strip mining and filling mining. The environmental core of green mining has distinct characteristics, such as the improvement of resource recovery, enhancement of mine safety and ecological environment protection of mining area. This is the main direction of scientific and technological development of the coal industry (Liu *et al.* 2018, Zhang *et al.* 2016, Xuan and Xu. 2017).

0.15~0.2 tons of coal gangue are produced by 1 t raw

coal production in China, and in 2013, 620 million tons of coal gangue were produced in China, accounting for about 40% of China's industrial solid waste. A large number of coal gangue have been piled up in the open-air, forming more than 2600 coal gangue hills with a cumulative stockpile of more than 5 billion tons, covering an area of more than 13333 km². It has become one of the industrial wastes with the largest storage amount, annual production and the largest number of accumulated sites in China (Guo *et al.* 2014, Zhang *et al.* 2017, Zhang and Meng. 2019).

To solve the major technical problems of coal pillar recovery and underground waste disposal, the way of coal pillar replacement with waste is used in coal mines. Based on the strip mining characteristics, Yu and Wang (2011) described the exchanging technology of gangue backfill according to strata movement and quadratic stability of coal-pillar. To analyze the overlying strata movement law of recovering room mining standing pillars with solid backfilling, An *et al.* (2016) conducted physical simulation experiments with sponge and wood as the backfilling simulation material.

In the compression process of gangue filling, the surrounding environmental factors include the overlying strata load, the groundwater, atmospheric precipitation and the later construction load will influence the compression process of gangue filling (Gu *et al.* 2018, Hu *et al.* 2018, Li *et al.* 2018). Gradation characteristics of filling waste affect the compression of gangue filling (Li *et al.* 2017). As a granular medium to fill the goaf, gangue filling has a significant impact on the movement of roof strata in coal mine because of special properties, especially the deformation characteristics of fractured rock mass (Li *et al.*

*Corresponding author, Ph.D.

E-mail: 723262355@qq.com

^aPh.D.

E-mail: 1554624100@qq.com

^bLecturer

E-mail: 1161826089@qq.com

^cM.Sc.

E-mail: 525047249@qq.com

^dM.Sc.

E-mail: 1033616923@qq.com

2016, Yan *et al.* 2018, Li *et al.* 2018). Compression ratio of the filling body is the most important indicator which is related to the final surface deformation. Zhou *et al.* (2017) designed and employed four experimental models for physical simulation, corresponding to roof-controlled backfilling ratios of 0%, 40%, 82.5% and 97% under geological conditions of workface No. 6304 in the Jining No. 3 coal mine, namely a solid backfill coal mining face under a hard roof.

In the above literature, theoretical, experimental and monitoring studies of gangue filling have been made to control the gangue filling subsidence. However, there are still some areas are required to be improved. For example, the test design of gangue compression deformation is inconsistent with the stress condition of the gangue filling. The test chamber of gangue compression is so small that the maximum particle size of crushed gangue sample is smaller, which is far from the actual particle size of on-site gangue filling. In order to obtain the compression deformation of gangue filling, a large-scale crushed rock compression test has been prepared in this paper, which can meet the maximum particle size of gangue compression in the field. The test material comes from the field filling gangue, and the loading mode simulates the stress process with the on-site filling gangue, and the relatively accurate deformation data can be obtained. In order to obtain the influence of groundwater on the compression deformation properties of gangue, two groups of comparative compression tests were carried out in natural state and saturated state. Finally, the prediction formula of surface subsidence of gangue filling is obtained and the experimental results and prediction formula are verified by the observation of surface rock movement in Xinwen Mining Area.

Xinwen Mining Area is located in Tai'an, Shandong Province, China, with a designed production capacity of 1.2 million t/a. In recent years, the output of raw coal in the mine has been more than 1.5 million tons. The fully mechanized gangue filling mining method is adopted in the working face of the No.7 mining area. The strike direction of the working face is 268-287° with an inclination of 358-17°. The dip angle is 6-9°, with the average of 7°. The roof is mainly composed of sandstone with a immediate roof is a sandstone of 1.7 m. The average thickness of coal seam is 1.7 m, the thickness of coal seam is stable.

2. Literature review of gangue filling effect

2.1 Roof mechanics model of gangue filling mining

When the roof is managed by the gangue filling mining method, the filling face that allows the free movement of the overlying strata has been filled with the gangue, and the immediate roof has been transformed into the main roof. With the advance of the working face, the basic roof breaks periodically. The hinged rock beam with different height is formed, as shown in Fig. 1 (An *et al.* 2016, Li *et al.* 2018, Yu *et al.* 2011, Venticinque *et al.* 2014).

Compared with coal body, the filling gangue has a obvious compressibility and the smaller strength. Thus, the main roof of the filling gangue under periodic fracture is regarded as an approximate cantilever beam. At the end of

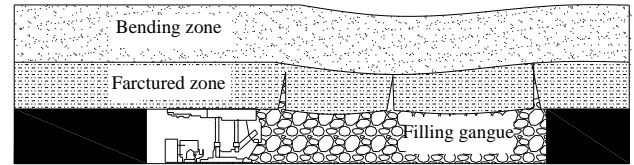


Fig. 1 Roof break rule of gangue filling working face

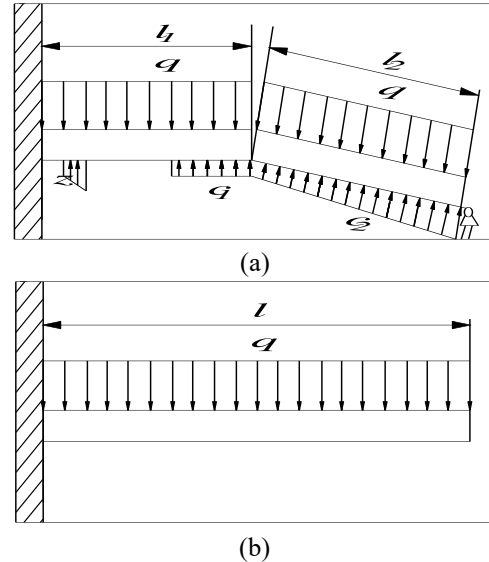


Fig. 2 Periodic press model of main roof in gangue filling mining working face

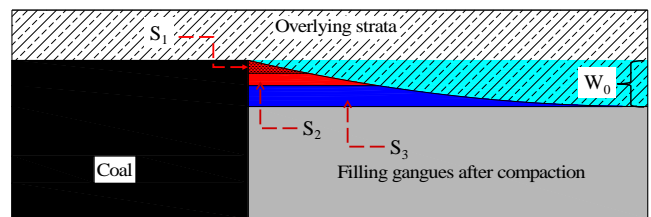


Fig. 3 Surface subsidence of gangue filling

the cantilever, supporting forces among the filling gangue c_1 , c_2 , the hydraulic support z_1 and the hinge force of the fractured rock beam are applied, as shown in Fig. 2(a).

Due to the following three factors: 1) With the increase of compression time, the strength of the filling gangue increases, and the rock beam l_2 subsidence increases, the supporting effect of filling gangue on rock beam l_2 is improved to a great extent. Therefore, the hinge effect of rock beam l_2 on rock beam l_1 is obviously weakened. 2) At this time, the supporting effect of filling gangue is much smaller than that of the gravity of the rock beam and the gravity of the overlying strata. 3) At this time, the supporting forces to the main roof is in the state of "given deformation", the supporting force has no effect on the final position of the rock beam, the supporting force only slows down the subsidence velocity. Then simplifies the main roof rock beam during the period of periodic compression to the form of the cantilever beam, as shown in Fig. 2(b). The main roof of the filling face is always supported by the filling gangue before and after the fracture, and the filling gangue is only compressed and deformed under the load of the overlying strata. Only when the settlement of the

cantilever end of the main roof reaches the maximum allowable limit, the main roof can fracture occur in front of the working face (Zhang *et al.* 2016, Zhang *et al.* 2019, Zhou *et al.* 2017, Jaouhar *et al.* 2018).

2.2 Theoretical analysis of deformation of gangue filling

Gangue filling in the goaf can effectively control surface subsidence caused by coal seam excavation, while it can not completely control the movement, deformation or destruction of overlying strata in the goaf. Because filling work always is performed after the coal mining operation. Surface subsidence occurs inevitably, namely the subsidence S_1 of roof before filling. It is difficult to fill the goaf completely by gangue filling, and non-filling amount S_2 directly leads to the roof subsidence. Coal gangue, as a bulk solid material, has a specific compression deformation, which is the compression amount S_3 of filling body. In addition, there are compression factors, including roof compression, floated coal compression and floor compression (Yavuz. 2004, Genis. 2018).

As shown in Fig. 3, the roof subsidence before filling (S_1), the non-filling amount (S_2) and the compression amount of filling body (S_3) are the main factors. Therefore, an equation of surface subsidence value W_0 can be simplified as Eq. (1)

$$W_0 = (S_1 + S_2 + S_3) \quad (1)$$

According to the above analysis, roof subsidence before filling (S_1) can be estimated by calculation formula of cantilever beam breaking. The immediate roof of No.7 mining area is a sandstone of 1.7 m, the elastic modulus of immediate roof $E=3500$ MPa, fracture step distance of rock beam l is 12.5 m, $\gamma=25$ kN/m³. Under the uniform load of overlying strata, the maximum deflection of the cantilever end of the cantilever beam can be calculated as 90.51 mm by Eq. (2).

$$S_1 = -\frac{ql^4}{8EI} = -\frac{3}{2} \frac{\gamma l^4}{Eh^2} \quad (2)$$

When conducting the gangue filling in the goaf, the solid gangue without water secretion can maintain a high roof-contacted rate. The non-filling amount is roughly equal to the particle size of the broken gangue. The particle size of the gangue filling is generally less than 60 mm, so the non-filling amount S_2 can be calculated as follows: $S_2=60$ mm.

The compression amount of filling body S_3 is mainly related to pre-compaction treatment before filling, particle graded of crushed gangue, impact of the surrounding environment, such as the pressure of surrounding rock, groundwater or seasonal precipitation. To obtain the reference value of S_3 , compression test of gangue filling is needed.

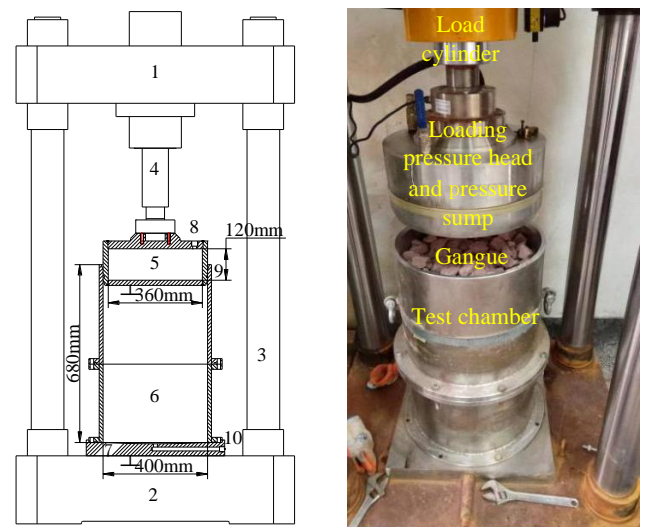
3. Experimental Method

3.1 Experimental system

The experimental control system consists of a console



Fig. 4 Testing control system (a) Console, (b) Hydraulic pressure double control servo system and (c) Displacement stress double control servo system



(a) System assembly diagram (b) System physical diagram

Fig. 5 Compression deformation seepage experimental system of fractured rock 1. Beam, 2. Base, 3. Column, 4. Load cylinder, 5. Loading pressure head and pressure sump, 6. Test chamber, 7. Beam of test chamber, 8. Water inlet, 9. Sealing ring, 10. Water (gas) mouth

Table 1 Major parameters of modified water and sand inrush simulation testing system

Axial compression	≤ 600 kN	Accuracy	0.01 kN
Water pressure	≤ 2 MPa	Accuracy	0.01 MPa
Displacement of hydraulic cylinder	≤ 500 mm	Accuracy	0.01 mm
Diameter of the test chamber	400 mm	Height	680 mm

and a servo loading system, the servo loading system consists of two parts: water pressure and quantity double control servo system and the displacement stress double control servo system, the whole process is automatic controlled by computer, the overall experimental control system is shown in Fig. 4. During the experiment, real-time monitoring and acquisition of displacement, load, water pressure and water quantity can be realized, the sampling

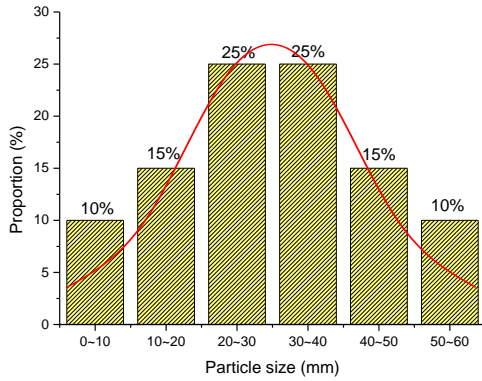


Fig. 6 Normal distribution of particle size

frequency can be set according to the different experimental contents.

Experimental loading and unloading system are shown in Fig. 5, the main parameters in Table 1.

3.2 Experimental scheme

The deformation of filling gangue is closely related to the stress, the early action of overlying strata on the gangue filling is mainly related to the movement space of the overlying strata in addition to its lithology. According to the movement theory of overlying strata, the early force of overlying strata on the backfill can be estimated by Eq. (3).

$$\sigma_z = \frac{\gamma S}{K_A - 1} \quad (3)$$

where S is the movement space of the overlying strata, namely the unfilled space, it is supposed as 0.5 m; γ is the overburden bulk density, KN/m^3 , here is 25 KN/m^3 ; K_A is the breaking expansion coefficient of partial caving overburden. K_A can be selected from 1.2 ~ 1.25 based on the prior experience. Therefore, the early force of the overlying strata on the backfill can be simplified as Eq. (4)

$$\sigma_z = (4 \sim 5)\gamma S \quad (4)$$

The calculated load on the gangue filling is about 0.06 MPa, and the later load is about 0.6 MPa for safety according to experience (State Administration of Coal Industry 2017). The diameter of the test chamber is 400 mm, so the maximum load is 100 KN. In order to increase the filling rate, pre-compaction loading is carried out.

When filling the goaf with gangue, the roof will not collapse, and the force acting on the gangue will increase linearly until it is equal to the gravity of overlying strata. Two groups of tests are designed. In a group of natural drying conditions, the preloading of 30 KN is carried out first, and then the axial load is increased to 100 KN by 0.5 kN/s loading rate, and the dry dead load test is conducted. In a group of soaking states, the pre-compaction loading of 20 KN is carried out first, and then the axial load is increased to 100 KN by 0.5 kN/s loading rate, and the immersion dead load test is performed.

According to the research of scholars (Zhang *et al.* 2013, Bishop and AlanW. 1962), considering the effect of

size effect, the ratio of sample diameter to rock maximum particle size should be ≥ 5 . Because the inner diameter of the test chamber is 40 cm, so the maximum diameter of rock is 80 mm. In order to minimize the effect of the size effect on the test results, the maximum particle size of the rock selected in the test is 60 mm. Compared with the existing test equipment, the effective dimension (diameter $\leq 150 \text{ mm}$, height $\leq 200 \text{ mm}$) has an obvious advantage in effective volume.

The maximum particle size in the compression deformation seepage experiment system is 60 mm, Therefore, the large blocks of fractured gangues are crushed and sieved into a total of 6 particle size groups, including 0 ~ 10mm, 10 ~ 20mm, 20 ~ 30mm, 30 ~ 40mm, 40 ~ 50mm and 50 ~ 60mm by the grading sieve. The proportion of fractured rock blocks is proportional to the normal distribution, as shown in Fig. 6.

4. Result analysis

4.1 Deformation behaviour characteristics analysis

The deformation curve and the coefficient of expansion are shown in Fig. 7. In a natural state, the height of original crushed gangue is 618 mm, the mass is 110 kg, the density is 25.60 kN/m^3 , and the initial coefficient of expansion is 1.81, the displacement is 105.06 mm, the strain of the whole stage is 0.17. In the loading stage, the strain is 0.15 and the displacement is 95.15 mm. The coefficient of expansion is 1.53. In the preloading stage, the strain is 0.04, the displacement is 27.50 mm, and the coefficient of expansion is 1.72. In the dead load stage, the strain is 0.02, the displacement is 9.91 mm, and the final coefficient of expansion is 1.50.

Under the soaking status, the height of the original crushed gangue is 620 mm, and the initial crushing expansion coefficient is 1.81, the displacement is 109.11mm, the strain of the whole stage is 0.18. The strain is 0.17 and the displacement is 103.28mm in the loading stage, and the coefficient of dilatation is 1.51. In the preloading stage, the strain is 0.03, the displacement is 19.48 mm and the coefficient of expansion is 1.75. In the dead load stage, the strain is 0.01, the displacement is 5.83mm, and the final coefficient of expansion is 1.49.

It can be clearly seen that in both natural and soaking states, the loading stage(OA, OA') (without preloading stage) presents the quadratic polynomial growth, and the dead load stage(AB, AB') presents the logarithmic growth. The fitting curve is shown by the blue line in the figure. The fitting determination coefficient R^2 is close to 1 with a great fitness. The curves of displacement at loading and dead load stages are shown in Figs. 8~11. The displacement and deformation in the natural loading stage account for 90.50% of the full deformation in the whole stage, while that in the soaking loading stage accounts for 94.65% of the total deformation in the whole stage, and the deformation in the dead load stage is small.

By comparison of data, the load gradient has a greater influence on the early deformation, while it has a smaller effect on the deformation in the dead load stage. Water has a

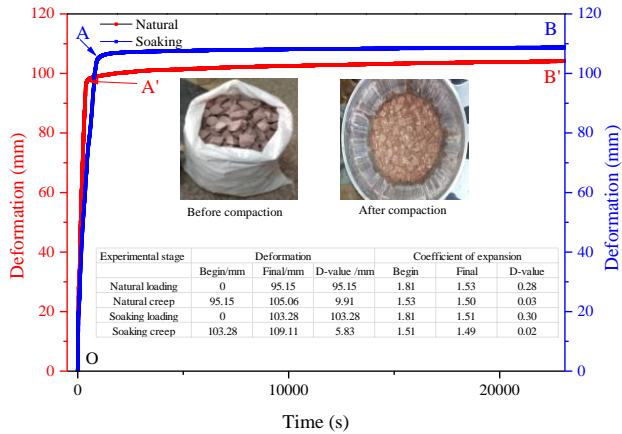


Fig. 7 Full scale curve under the natural-soaking condition

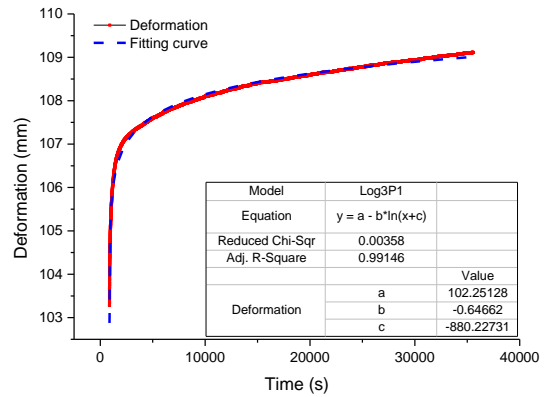


Fig. 11 Dead load stage curve under soaking state

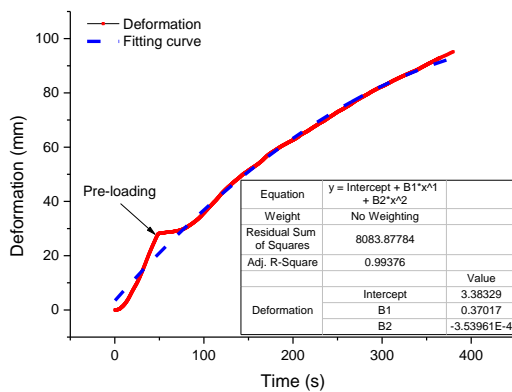


Fig. 8 Loading stage curve under natural state

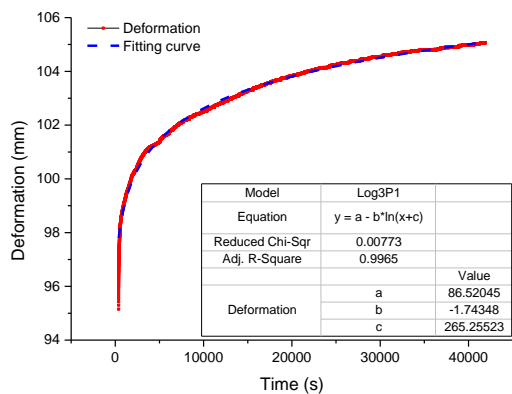


Fig. 9 Dead load stage curve under natural state

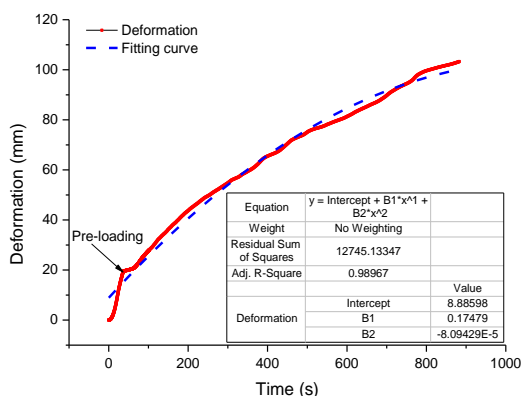


Fig. 10 Loading stage curve under soaking state

greater impact on the deformation in the dead load stage, while it has a smaller effect on the early deformation. This is mainly caused by different forms of deformation of crushed gangue in the early and later stages. Therefore, the load gradient and water play different roles in different stages. The early stage is mainly composed of the sliding deformation caused by the position adjustment, which does not require too much external force to make the slide deformation of fractured rock. In the later stage, it is mainly composed of further fracture and compression deformation of the broken rock. When the load gradient reaches the maximum value, under the dual action of water lubrication and softening, the fractured rock is broken more fully with denser filling.

In summary, total deformations of the two groups are similar, and water plays an important role in accelerating the compression process. With the roof bends gradually, the load gradient on the gangue increases, and there is a large deformation in the early stage of gangue filling. Hence, the gangue should be precompacted or strengthened by grouting. In the later stage of gangue filling, there is a stable deformation. However, when groundwater reciprocates or seasonal precipitation occur, the deformation may increase suddenly in the goaf, resulting in the activation of the stable old goaf and surface deformation. So the real-time monitoring is required for the evaluation.

When the gangue fills the goaf, the roof contacts with the gangue in the process of deformation, and pressure yield until the position of the crushed gangue is adjusted. After the initial compaction, the gangue plays a supporting role on the roof. To avoid the large deformation in the early stage of filling, it is necessary to pre-compact the gangue and maintain a certain strength and action time.

4.2 Energy dissipation characteristics analysis

In the process of compaction, the crushed rock void closure, the friction slip and the extrusion failure are all needed to dissipate energy, and the friction between the crushed rock and the cylinder wall also needs to dissipate energy. As the test machine is stiff loading machine, so the work of the testing machine on the crushed rock is the energy dissipated by the crushed rock (Zhang, 2008). The work done by the testing machine on the unit volume crushed rock can be expressed as Eq. (5)

$$W_Z = \int_0^{\varepsilon_a} \sigma d\varepsilon \quad (5)$$

It should be noted that the axial compaction stress consists of a part of the friction between the crushed rock and the steel cylinder. When the axial compaction stress is σ , the lateral stress is $\sigma_b = \lambda\sigma$ caused by the obstruction of lateral deformation. According to the experimental results carried out by many researchers, the lateral pressure coefficient is 0.43, so in this paper, the lateral pressure coefficient λ is taken 0.43 (Miao *et al.* 1997). The resulting friction is $\mu\lambda\sigma(\pi DH)$, μ is coefficient of friction between broken rock and side wall, approximately 0.25 (Su *et al.* 2012), based on which the energy dissipation of friction between crushed stone and steel cylinder is estimated as Eq. (6)

$$W_m = \int_0^{\varepsilon_a} \mu\lambda\sigma\pi DH \frac{Hd\varepsilon}{2} = 2\mu\lambda \frac{H}{D} W_Z \quad (6)$$

In the formula: H , D is crushed rock height and diameter respectively. Under the natural condition, $H=618$ mm, $H/D=1.545$, 33% of the work done by the compaction load is used for friction energy dissipation between crushed stone and cylinder wall, 67% is used to close the void, friction slip and extrusion failure between the crushed stones can be called crushing energy dissipation. Under the condition of saturated water, $H=620$ mm, $H/D=1.55$, the energy dissipation of friction between crushed stone and cylinder wall is 33% of the work of compaction load, and 67% is used to close the void of crushed stone, friction slip between crushed stone, and extrusion failure. It can be seen that different water-bearing states have little effect on the energy dissipation of crushed stone compression friction and crushing.

From Fig. 12 and Table 2, we can find that in natural state, the strain of OA' loading stage is about 88% of the total strain, and the energy dissipation is about 74% of the total energy dissipation. Under saturated water condition, the strain of OA at loading stage accounts for 94% of the total strain, and the energy dissipation accounts for 91% of the total energy dissipation. The results show that in the loading stage, the void closure increases faster, the energy dissipation is relatively less, and the energy dissipation changes relatively slowly. Although the crushing gangue accelerates the deformation under the condition of saturated water, the energy dissipation increases accordingly. In natural state, the strain of AB' dead load stage accounts for about 12% of the total strain, and the energy dissipation accounts for about 26% of the total energy dissipation. Under saturated water, the strain of AB dead load stage accounts for about 6% of the total strain, and the energy dissipation accounts for about 9% of the total energy dissipation. It shows that during the dead load stage, the larger rock mass rotates and moves to a close contact state, forming a stable structure, and more work is needed to achieve further compression of the broken rock. It can be seen that loading mode determines the rate of change of energy consumption in different stages, and different water-bearing states have an important influence on energy consumption in different stages.

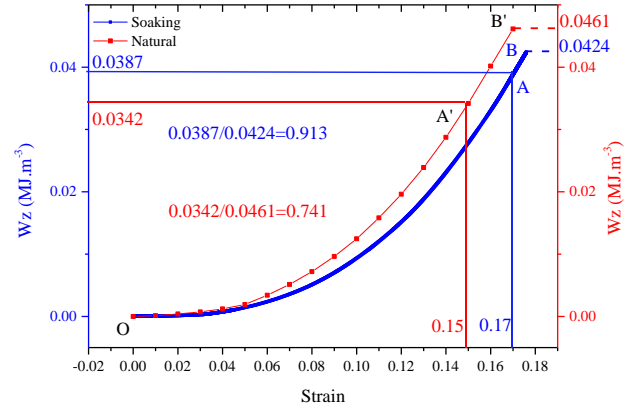


Fig. 12 Energy dissipation of crushed stones during compaction process

Table 2 Energy dissipation rate-strain in different stages

State	OB	OB	OA	OA	OA	OA	AB	AB	AB	AB
	Strain	E-d Strain	Strain	S- Ratio	E-d (MJ.m-3)	E- Ratio	Strain	S- Ratio	E-d (MJ.m-3)	E- Ratio
Natural	0.17	0.0461	0.15	88	0.0342	74	0.02	12	0.0119	26
Soaking	0.18	0.0424	0.17	94	0.0387	91	0.01	6	0.0037	9

Note: E-d is energy dissipation, in a natural state, OB is OB', OA is OA', AB is AB'

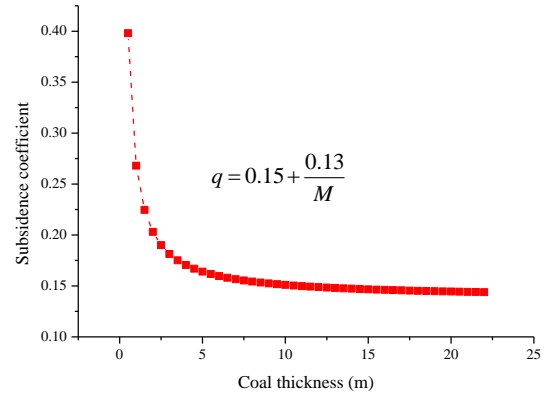


Fig. 13 Surface subsidence coefficient prediction along with mining thickness

4.3 Prediction of subsidence coefficient of gangue filling

The compression amount of filling gangue (S_3) can be regarded as the total displacement of gangue filling after the stable dead load compression. The compression ratio is equivalent to the total strain minus the pre-loaded strain. The calculation result is 0.15, so the compression rate of gangue filling is

$$S_3 = 0.15h_g \quad (7)$$

where h_g is the filling height of gangue, m.

The roof subsidence before filling is $S_1=90.51$ mm. The non-filling amount of gangue filling (S_2) can be calculated as follows: $S_2=60$ mm. The compression amount of gangue filling is

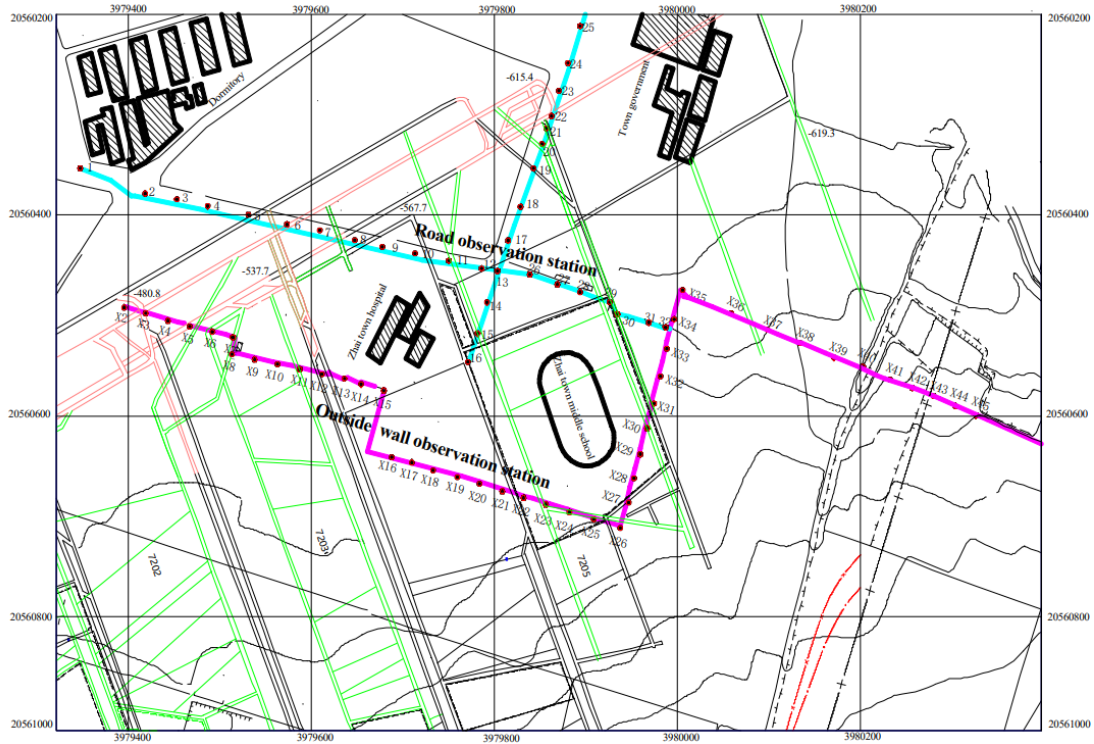


Fig. 14 Layout plan for observation stations in No.7 mining areas

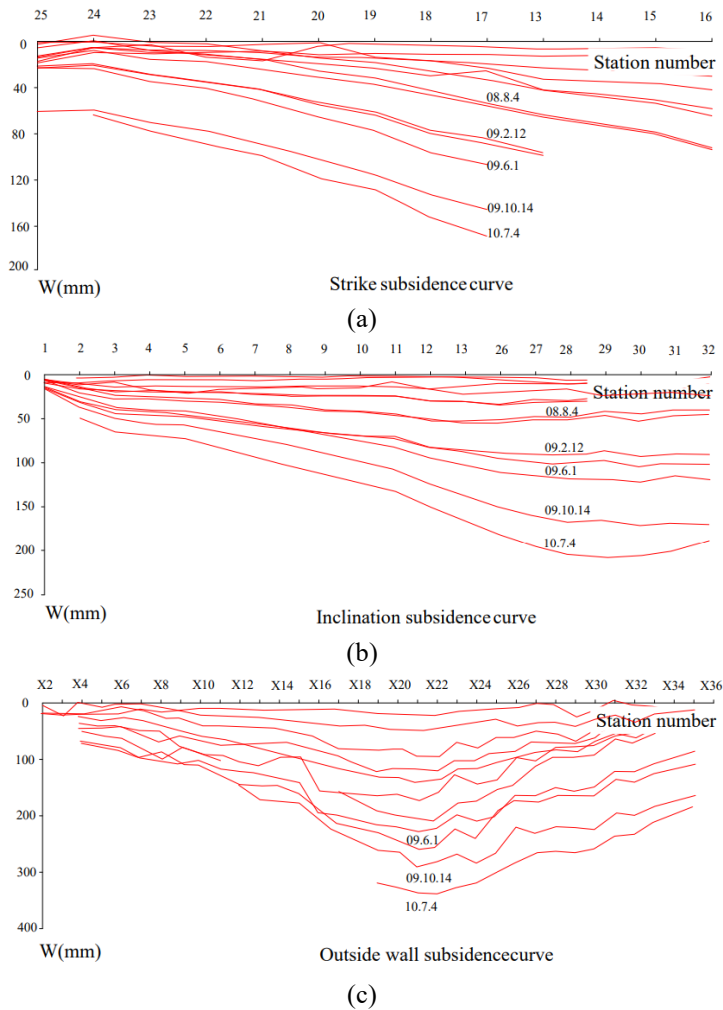


Fig. 15 Subsidence curve of No.7 mining observation station

$$S_3 = 0.15h_g = 0.15(M-0.15) \quad (8)$$

where M is the mining height, m.

In the form, the total subsidence of gangue filling is estimated as

$$W_0 = 0.15M + 0.13 \quad (9)$$

The subsidence coefficient of the surface is estimated as

$$q = 0.15 + \frac{0.13}{M} \quad (10)$$

Through Eq. (10) and Fig. 13, we can draw that: when the mining thickness is less than 5 m, the subsidence coefficient of the surface varies greatly with the mining thickness, and when the mining thickness exceeds 4 m and continues to increase, the subsidence coefficient of the surface is stable at about 0.15.

According to the above prediction formula, the surface subsidence of No. 7 mining area is calculated as 431 mm, the subsidence coefficient of the surface is 0.26.

5. Monitoring of gangue filling effect

5.1 Layout of surface strata observation stations in No. 7 mining area

The effect of gangue filling mining is determined by observing the surface movement and deformation. According to the ground characteristics of No. 7 mining areas, it is impossible to lay observation points on the buildings due to the difficulty of observation. Therefore, two observation lines are set up based on the actual conditions of the surface, surrounding walls and roads. The distance between the road observation stations and the observation stations outside the walls is about 28m. There are 32 observation points in the road observation stations and 45 observation points of observation stations outside the walls. The layout of observation stations in No.7 mining areas are shown in Fig. 14. According to the parameters of surface movement and deformation obtained from previous observation stations in coal mines, the parameters adopted in the design of observation stations are: strike movement angle, $\alpha=70^\circ$; uphill movement angle, $\gamma=70^\circ$; downhill movement angle, $\alpha=64^\circ$; maximum subsidence coefficient, $q=0.6$; horizontal displacement coefficient, $b=0.33$.

5.2 Results of observation analysis

During the observation period, 14 times observations were carried out on the observation lines. Fig. 15 shows subsidence curves. Through comprehensive analysis and calculation, parameters of strata movement under filling mining are obtained as follows: subsidence coefficient, $q=0.30$; horizontal displacement coefficient, $b=0.28$; tangent of major influence angle, $tg\beta_1=2.0$, $tg\beta_2=1.85$; the inflection point displacement distance, $S=0.036H$. The subsidence coefficient is quite close to the prediction.

Table 3 Parameters of rock movement in filling mining in Xinwen Mining Area

Mine name	Filling mode	Coal thickness (m)	q	q-estimated
Huaheng	Gangue paste filling	1.4	0.08	0.24
Liangzhuan g	Gangue consolidation filling	1.9	0.13	0.22
Shengquan	Water sand gangue filling	1.2	0.13	0.26
Xiezhuang	Raw gangue throwing filling	2.7	0.14	0.20
Panxi	Fully mechanized gangue filling	2.3	0.15	0.21
Ezhuang	Fully mechanized gangue filling	1.6	0.17	0.23
Zhangzhuan g	Gangue paste filling	1.4	0.22	0.24
Suncun	Raw gangue throwing filling	2.0	0.23	0.22
Zhaizhen	Gangue consolidation filling	1.6	0.30	0.23

5.3 Surface movement parameters of filling mine in Xinwen Mining Area

After gangue filling or gangue cemented filling mining, the surface movement parameters of Xinwen mining area are shown in Table 3. As can be seen from Table 3 (Guo, 2013), the coefficient of surface subsidence q concentrates between 0.08 ~ 0.30, relatively discrete. The predicted subsidence coefficient is between 0.20 ~ 0.26, which is relatively concentrated. The upper limit deviations of the predicted subsidence values are small and lower limit deviations of the predicted subsidence values are large. This is because the gap between gangue is filled with external cementing material or sand body at the same time.

6. Conclusions

- When gangue fills the goaf, there are three main factors which influence the surface subsidence for gangue filling method, namely the roof subsidence before filling, non-filling amount and the compression amount of gangue filling. The roof subsidence before filling is estimated by calculation formula of cantilever beam breaking. The non-filling amount is roughly equal to the maximum particle size of gangue filling, and the particle size of gangue filling is generally less than 60 mm.

- In the loading stage, the deformation is significant. At this stage, the structure adjustment is dominant among the broken rock particles accompanying by the breakage of broken rock edges. In the dead load stage, although the impact compaction of broken rock is over, the redistribution of stress between particles will also lead to the breakage and refinement of the angular or weak particles, and the sliding and arrangement of particles will be further adjusted, showing slow deformation on the macro scale.

- Different water-bearing states have little effect on the energy dissipation of crushed stone compression friction and crushing. In the loading stage, deformation is fast but energy dissipation is relatively low. In the dead load stage, deformation is slow but energy dissipation is relatively fast. The compression amount of backfilling gangue is

approximately equal to 0.15 of the filling height, so the subsidence coefficient of the gangue filling is estimated by a statistical formula proposed.

Acknowledgments

This work was supported by Taishan Scholar Talent Team Support Plan for Advantaged & Unique Discipline Areas and Open Fund of State Key Laboratory of Water Resource Protection and Utilization in Coal Mining (Grant No. SHJT-17-42.14); Key research and development plan of Shandong Province (2018GSF120003) and National Natural Science Foundation of China (51804179).

References

- An, B., Miao, X., Zhang, J., Ju, F. and Zhou, N. (2016), "Overlying strata movement of recovering standing pillars with solid backfilling by physical simulation", *Int. J. Min. Sci. Technol.*, **26**(2), 301-307. <https://doi.org/10.1016/j.ijmst.2015.12.017>.
- Bishop, A.W. and Henkel, D.J. (1962), *The Measurement of Soil Properties in the Triaxial Test*, Edward Arnold Ltd., London, U.K.
- Genis, M., Akcin, H. and Aydan, O. (2018), "Investigation of possible causes of sinkhole incident at the Zonguldak Coal Basin, Turkey", *Geomech. Eng.*, **16**(2), 177-185. <https://doi.org/10.12989/gae.2018.16.2.177>.
- Ghabraie, B., Ren, G., Barbato, J. and Smith, J.V. (2017), "A predictive methodology for multi-seam mining induced subsidence", *Int. J. Rock Mech. Min. Sci.*, **93**, 280-294. <https://doi.org/10.1016/j.ijrmm.2017.02.003>.
- Gu, H., Tao, M., Wang, J., Jiang, H., Li, Q. and Wang, W. (2018), "Influence of water content on dynamic mechanical properties of coal", *Geomech. Eng.*, **16**(2), 85-95. <https://doi.org/10.12989/gae.2018.16.2.085>.
- Guo, W. (2013), *Backfill Mining Technology in Coal Mines*, China Coal Industry Publishing House, Beijing, China.
- Guo, Y., Zhang, Y.Y. and Cheng, F.Q. (2014), "Industrial development and prospect about comprehensive utilization of coal gangue", *Ciesc J.*, **65**(7), 2443-2453.
- Hu, C.M., Wang, X.Y., Mei, Y., Yuan, Y.L. and Zhang, S.S. (2018), "Compaction techniques and construction parameters of loess as filling material", *Geomech. Eng.*, **15**(6), 1143-1151. <https://doi.org/10.12989/gae.2018.15.6.1143>.
- Ishwar, S.G. and Kumar, D. (2017), "Application of DInSAR in mine surface subsidence monitoring and prediction", *Curr. Sci.*, **112**(1), 46-51.
- Jaouhar, E.M., Li, L. and Aubertin, M. (2018), "An analytical solution for estimating the stresses in vertical backfilled stopes based on a circular arc distribution", *Geomech. Eng.*, **15**(3), 889-898. <https://doi.org/10.12989/gae.2018.15.3.889>.
- Ju, J. and Xu, J. (2015), "Surface stepped subsidence related to top-coal caving longwall mining of extremely thick coal seam under shallow cover", *Int. J. Rock Mech. Min. Sci.*, **78**, 27-35. <http://dx.doi.org/10.1016%2Fj.ijrmm.2015.05.003>
- Li, J., Huang, Y., Qiao, M., Chen, Z., Song, T., Kong, G., Gao, H. and Guo, L. (2018), "Effects of water soaked height on the deformation and crushing characteristics of loose gangue backfill material in solid backfill coal mining", *Processes*, **6**(6), 64. <https://doi.org/10.3390/pr6060064>.
- Li, M., Zhang, J. and Gao, R. (2016), "Compression characteristics of solid wastes as backfill materials", *Adv. Mater. Sci. Eng.*, 1-7. <http://dx.doi.org/10.1155/2016/2496194>.
- Li, M., Zhang, J., Huang, Y. and Zhou, N. (2017), "Effects of particle size of crushed gangue backfill materials on surface subsidence and its application under buildings", *Environ. Earth Sci.*, **76**(17), 603. <https://doi.org/10.1007/s12665-017-6931-z>.
- Li, Y., Zhang, S. and Zhang, X. (2018), "Classification and fractal characteristics of coal rock fragments under uniaxial cyclic loading conditions", *Arab. J. Geosci.*, **11**, 201-212. <https://doi.org/10.1007/s12517-018-3534-2>.
- Liu, X.S., Ning, J.G., Tan, Y.L., Xu, Q. and Fan, D.Y. (2018), "Coordinated supporting method of gob-side entry retaining in coal mines and a case study with hard roof", *Geomech. Eng.*, **15**(6), 1173-1182. <https://doi.org/10.12989/gae.2018.15.6.1173>.
- Miao, X.X., Mao, X.B., Hu, G.W. and Ma, Z.G. (1997), "Research on broken expand and press solid characteristics of rocks and coals", *J. Exp. Mech.*, **12**(3), 394-399.
- Shen, B. and Barton, N. (2018), "Rock fracturing mechanisms around underground openings", *Geomech. Eng.*, **16**(1), 35-47. <https://doi.org/10.12989/gae.2018.16.1.035>.
- State Administration of Coal Industry (2017), *Regulations for the Preservation and Mining of Coal Pillars in Buildings, Water Bodies, Railways and Main Roadways*, Coal Industry Publishing House, Beijing, China.
- Su, C.D., Gu, M., Tang, X. and Guo, W.B. (2012), "Experiment study of compaction characteristics of crushed stones from coal seam roof", *Chin. J. Rock Mech. Eng.*, **31**(1), 18-26.
- Venticinque, G., Nemcik, J. and Ren, T. (2014), "A new fracture model for the prediction of longwall caving characteristics", *Int. J. Min. Sci. Technol.*, **24**(3), 369-372. <https://doi.org/10.1016/j.ijmst.2014.03.014>.
- Xuan, D. and Xu, J. (2017), "Longwall surface subsidence control by technology of isolated overburden grout injection", *Int. J. Rock Mech. Min. Sci. Technol.*, **27**(5), 813-818. <https://doi.org/10.1016/j.ijmst.2017.07.014>.
- Yan, C., Wan, Q., Xu, Y., Xie, Y. and Yin, P. (2018), "Experimental study of barrier effect on moisture movement and mechanical behaviors of loess soil", *Eng. Geol.*, **240**, 1-9. <https://doi.org/10.1016/j.enggeo.2018.04.007>.
- Yavuz, H. (2004), "An estimation method for cover pressure re-establishment distance and pressure distribution in the goaf of longwall coal mines", *Int. J. Rock Mech. Min. Sci.*, **41**(2), 193-205. [https://doi.org/10.1016/S1365-1609\(03\)00082-0](https://doi.org/10.1016/S1365-1609(03)00082-0).
- Yu, W.J. and Wang, W.J. (2011), "Strata movement induced by coal-pillar under three circumstances exchanged by gangue backfill and quadratic stability law", *Chin. J. Rock Mech. Eng.*, **30**(1), 105-112.
- Zhang, C., Zhan, X. and Yang, C. (2013), "Mesoscopic simulation of strength and deformation characteristics of coarse grained materials", *Rock Soil Mech.*, **34**(7), 2077-2083.
- Zhang, J., Li, B., Zhou, N. and Zhang, Q. (2016), "Application of solid backfilling to reduce hard-roof caving and longwall coal face burst potential", *Int. J. Rock Mech. Min. Sci.*, **88**, 197-205.
- Zhang, X., Lin, J., Liu, J., Li, F. and Pang, Z. (2017), "Investigation of hydraulic-mechanical properties of paste backfill containing coal gangue-fly ash and its application in an underground coal mine", *Energies*, **10**(9), 1309. <https://doi.org/10.3390/en10091309>.
- Zhang, Z. (2008), "Analysis of plastic deformation and energy property of marble under pseudo-triaxial compression", *Chin. J. Rock Mech. Eng.*, **27**(2), 273-280.
- Zhang, B. and Meng, Z. (2019), "Experimental study on floor failure of coal mining above confined water", *Arab. J. Geosci.*, **12**(4), 114-123. <https://doi.org/10.1007/s12517-019-4250-2>.
- Zhang, S., Li, Y., Shen, B., Sun, X. and Gao, L. (2019), "Effective evaluation of pressure relief drilling for reducing rock bursts and its application in underground coal mines", *Int. J. Rock Mech. Min. Sci.*, **114**, 7-16. <https://doi.org/10.1016/j.ijrmm.2018.12.010>.

Zhou, N., Zhang, J., Yan, H. and Li, M. (2017), "Deformation behavior of hard roofs in solid backfill coal mining using physical models", *Energies*, **10**(4), 557. <https://doi.org/10.3390/en10040557>.

GC